OLEIC FATTY ACID AND CARBONIZED BAMBARA NUTSHELL CATALYST IN THE OPTIMIZATION OF BIODIESEL PRODUCTION USING DOE PRO XL

Kefas, H.M.[1*], Silas, K.[2], Abubakar, A.M.[1] and Titus, A.[1]

[1]Department of Chemical Engineering, Faculty of Engineering, Modibbo Adama University, Yola, Adamawa State, Nigeria

[2]Department of Chemical Engineering, Faculty of Engineering, University of Maiduguri, Maiduguri, Borno State, Nigeria

*Corresponding email: hmkefas@mau.edu.ng

ABSTRACT

Decades of study have favored the utilization of oleic acid (OA) as an efficient free fatty acid (FFA) for biodiesel (Fatty Acid Methyl Ether–FAME) production via esterification/transesterification synthesis routes, without utilizing Bambara Nut Shell (BNS) as catalyst. The aim of this study is to optimize FAME production by varying the methanol (CH_3OH)/oil molar ratio (8:1-12:1), reaction time (60-180 min), and catalyst weight (1-4 wt.%) using Design of Experiments (DOE) Pro XL Version 21.00.000, with a focus on utilizing BNS as a catalyst for the esterification process. Fourier Transform Infrared (FTIR) spectroscopy and Scanning Electron Microscope (SEM) were objectively employed to identify the functional groups and morphology of the BNS material that allow for its usage as esterification catalyst. A 2D interaction, 3D surfaces and contours plots were analyzed using the software for the response variable sensitivity to the 3 parameters. At a sulfonation temperature of 130℃ and a constant reaction temperature of 65℃, a 20 run observed data under full factorial design, respectively pinpoints at 11.05:1 CH_3OH/oil ratio, 122.37 min time and 3.15 wt.% catalyst concentration as the optimal factors. It corresponds to 98.27% optimum FAME conversion in line with a quadratic model, which provided up to 96.06% experimentally verified value. Residual analysis revealed that data points with higher leverage often exhibit larger residuals and higher Cook's D values, suggesting that these points are more influential and could potentially skew the regression model's results. From the forgone results, it was discovered that BNS catalyst was efficient in the production of biodiesel using OA and will potentially convert feedstock with high fatty acid. Further research could focus on optimizing these parameters for different feedstocks to improve biodiesel yield and process efficiency.

Keywords: Bambara nutshell, Catalyst synthesis, Oleic acid, Biodiesel optimization, DOE Pro XL

1 INTRODUCTION

Bambara nut shells (BNS) can be used as catalyst in the esterification of CH_3OH to produce FAME. BNL possess several properties that make them suitable for biodiesel production, particularly as a source of biomass for catalytic materials. The shells are rich in lignocellulosic content, which can be processed into biochar and activated carbon. These materials can then be utilized as catalysts or catalyst supports in the transesterification process to produce biodiesel. Additionally, the high surface area and porosity of activated carbon derived from BNSs enhance their catalytic activity, improving the efficiency of biodiesel production. Furthermore, the shells are an abundant agricultural waste product, offering a low-cost and sustainable raw material that contributes to waste valorization. Utilizing BNSs in biodiesel

production not only provides a renewable energy source but also supports environmental sustainability by reducing agricultural waste and promoting the circular economy. Most especially, in Nigeria having diverse biomass waste for potential utilization as ingredients of biofuel production, as researched by [1]. Oleic acid (OA) is the most common acid employed in the conversion of CH_3OH to biodiesel. Its choice in this study, is due to its lower freezing point, enhanced biodiesel stability and higher reactivity in esterification. Thus, OA is more favorable than linoleic, linolenic, palmitic and stearic acid, judging by the aforementioned characteristics. Design-Expert® (DOE Pro XL) is a robust software used for design of experiments (DOE) and statistical analysis, widely applied in engineering, manufacturing, and scientific research to optimize processes, improve quality, and gain insights into complex systems. It offers a variety of experimental designs such as factorial, response surface, mixture, and combined designs, alongside tools for statistical analysis including analysis of variance (ANOVA), regression, and model diagnostics. The software aids in identifying optimal conditions for processes or product performance through response surface methodology (RSM) and other optimization techniques. With powerful graphical tools for visualizing data and results, such as contour plots, 3D surfaces plots, and interaction plots, DOE Pro XL is designed to be intuitive and user-friendly, even for those without extensive statistical backgrounds, enhancing the efficiency and effectiveness of experimental studies. In this study, effects of varying CH_3OH/OA ratio, reaction time and catalyst weight, was experimented and analyzed using DOE Pro XL for optimal FAME production. In several reports in the literature, these 3 parameters have been proven to be influential in biodiesel production. DOE Pro XL Excel add-in offers an additional/unique output such as marginal means plot, skeletal/line depiction of the 3D surface plot and 2D interaction line plots. These special features are not found in other optimization tools like Minitab, Stat-Ease 360 Design Expert, SigmaXL and JMP. Moreso, the software was adapted for this analysis because of the simplicity it offers in finding the optimal combinations, as demonstrated in few previous utilizations [2, 3, 4, 5, 6, 7]. Basically, the present study adds to several catalyst used previously, thereby diversifying the precursors employed for FAME production, to compliment OA and CH_3OH that have been used consistently for decades. Generally, optimizing the synthesis of biodiesel production has been the main goal in several studies.

2 MATERIALS AND METHOD

2.1 Materials, BNS Collection and Cleaning

Oleic fatty acid was purchased from Onitcha, Anambra State, Nigeria. Without the need for purification, analytical grade chemicals were utilized in this experimental study. They include CH_3OH, sodium hydroxide (NaOH), concentrated H_2SO_4 and phenolphthalein solution. Glassware and containers were washed with liquid detergent and rinsed with distilled water. There was also the rinsing of the containers with appropriate reagents before utilization. Surface impurities were removed from the collected BNS by washing it. It was then placed in an air-blast drying oven at 105℃ to vent-off moisture. BNS was grinded and sieved to particle size of 0.125 mm.

2.2 Carbonization of BNS and Sulfonation

Certain amount of BNS powder was put into the furnace under an inert atmosphere for 60 min at a temperature of 250℃. About 40g of BNS biochar was mixed with 100 mL of concentrated H_2SO_4 and heated in an oil bath at 130℃ specific sulfonation temperature. It was stirred with magnetic stirrer for 8 h under nitrogen flow. The sample was later diluted with distilled water and washed to remove excess acid and impurities. It was subsequently dried at 105℃ in an oven to remove the absorbed water molecules for 720 min and kept for further analysis. This stage is based on previous study by [8].

2.3 FTIR and SEM Characterization

Chemical composition of the BNS solid residues, char and catalyst activated, were analyzed using Fourier transform infra-red (FTIR) machine, as conducted by [9]. Specifically, functional group analysis of sulfonate group (SO_3H) was conducted using FTIR research instrument Shimadzu (FTIR-8400). Scanning electron microscope (SEM) analysis was carried out to determine the morphology of the catalyst surface.

2.4 Bench-Scale Biodiesel Production

OA and CH_3OH were added to a 250 mL reaction vessel under continued agitation until temperature of about 65℃ was attained. Then, heterogeneous acid catalyst was put into the reaction vessel to start the reaction using magnetic stirrer. When the reaction time was attained, the magnetic stirrer was put off to stop the reaction and the product was transferred into a vessel to cool to normal (room) temperature. It was then centrifuged to separate the product from the catalyst, in layers.

2.5 FFA Determination

FFA of the OA was determined using Official Methods and Recommended Practices of the AOCS [10]. Certain amount of oleic fatty acid was weighed into a conical flask and 25 mL distillation. The catalytic performance of the BNS-based heterogeneous acid catalysts was calculated. Ethanol was added to the flask. Approximately 3 drops of phenolphthalein solution were added to the mixture and titrated against 0.1N NaOH solution to a steady pink end point. The procedure was repeated and the average titrated value of the NaOH used was recorded, when the precision of each run does not exceed 0.1. Thus, the FFA of the sample was calculated using Equation 1, while the FAME conversion using Equation 2 [11].

$$\text{FFA}(\%) = \frac{28.2(\text{Volume of Titre Value})(0.1\text{N NaOH})}{\text{Weight of Oil Used}} \times 100 \quad (1)$$

$$\text{Ester Conv.}(\%) = \frac{\text{FFA}_{\text{Control}} - \text{FFA}_{\text{Test}}}{\text{FFA}_{\text{Control}}} \times 100 \quad (2)$$

Where 28.2 is the molecular weight of OA. FFA contents were specified as the test system and the control, respectively.

2.6 DOE Pro XL Numerical Analysis

2.6.1 Design, Factor Specification and ANOVA

A Microsoft Excel menu bar add-in known as DOE Pro XL 2021, developed by Sigma Zone (Digital Computations, Inc.) and Air Academy Associates, LLC, was used to optimize the production of biodiesel. 'Computer Aided Design' was selected under 'Create Design' drop-down under the Sigma Zone menu option. Number of levels (i.e., 2) with 3 factors (8 Run Full Factorial) design was chosen. In this case, factors A, B and C were respectively tagged CH_3OH/oil ratio, catalyst weight (%) and reaction time (min). Afterwards, 'Next' was clicked and the number of responses (i.e., 1) was specified. In the present study, FAME conversion (%) is the desired response. Exactly 1 number of replicates was specified and 'Next' was clicked, before entering the response name and clicking on 'Finished'. By default, 8 runs are shown in the DOE Pro XL spreadsheet. To change the number of runs, 'Modify Design' dropdown sub-menu was entered and 20 runs was specified. Under the same dropdown, all quadratic interactions were added. Regression model table for the actual (uncoded) coefficient, and ANOVA and marginal means plot for the FAME conversion were created under the 'Analyze Design' dropdown menu.

2.6.2 Interactions, Surface and Contour Plots

Interaction, 3D-interaction, surface and contour plots for the response data was generated under the 'Graphs and Optimization' dropdown, by choosing the coded response coefficient sheet. Again, by choosing the coded sheet as the reference sheet, optimization was carried out. Under the same dropdown sub-menu, the Y-hat Pareto of coefficients chat for the FAME efficiency was generated.

2.6.3 Y-hat Residuals

The residual sheet was generated by clicking on 'Generate Residual Sheet' from the 'Residual Analysis' dropdown sub-menu under Sigma Zone. 'Residual Plots' was entered in order to plot the Predicted Y versus Actual Y, as well as the Residual versus Actual Y plots. Note that 'Y' here implies biodiesel conversion.

3 RESULTS AND DISCUSSION

3.1 Sulfonate Group Presence Analysis

FTIR analysis reveals the presence of several functional groups that are contributory to the production of biodiesel. Sulfonate group (SO_3H) is essential for the esterification process in biodiesel production [12, 13, 14]. Their peaks are typically found in the range of 1000-1200 cm^{-1}, indicative of the S=O stretching vibration [15], as discussed by [16]. Secondly and as reported by [17, 18], the carboxyl group (COOH) found around 1700 cm^{-1}, also plays a role in the esterification process. In Figure 1, peaks near 3300-3600 cm^{-1} are indicative of hydroxyl groups, which are crucial for catalytic activity in biodiesel synthesis. In comparison, the BNS catalyst shows more pronounced peaks for the sulfonate groups, which are essential for biodiesel production. The catalyst also shows higher peaks at wavenumbers around 1166.5051 and 2954.4404 cm^{-1} (Figure 1a) compared to the char (Figure 1b), indicating the presence of active functional groups.

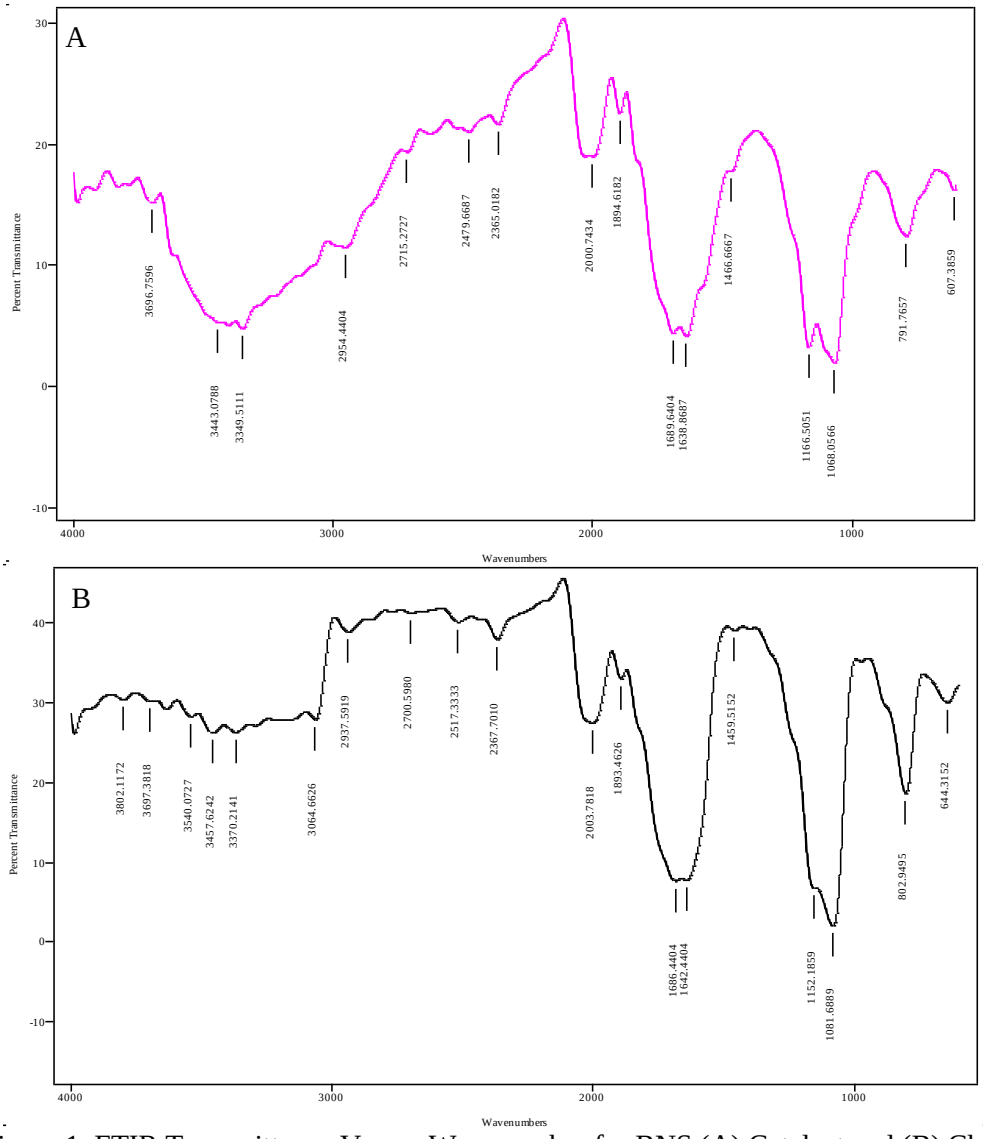

Figure 1. FTIR Transmittance Versus Wavenumber for BNS (A) Catalyst and (B) Char

On the other hand, the char has higher peaks at certain wavenumbers such as 1642.4404 and 2517.3333 cm^{-1} (Table 1), but these are not as influential in the esterification process as the sulfonate groups found in the catalyst. Peak at 3697.3818 cm^{-1}, found in the char but not significantly high in the catalyst,

may indicate hydroxyl groups that are not directly influential in the biodiesel conversion process [19]. But it plays a crucial role in the preparatory stages of the catalyst formation and activation. Generally, the presence of hydroxyl groups can influence the hydrophilicity and acid-base properties of the catalyst, thereby affecting the overall catalytic activity indirectly. Though absent, the presence of methoxy groups could be beneficial in enhancing the catalyst's performance for biodiesel production. These groups typically show peaks around 2800-3000 cm^{-1}. It is obvious that the BNS catalyst shows promise for biodiesel production, as revealed by Figure 1a FTIR analysis, but further optimization and characterization are recommended to achieve the best results.

Table 1. BNS Catalyst and Biochar Peak Height and Wavenumbers

BNS Catalyst		BNS Char	
Peak At	Peak Height	Peak At	Peak Height
607.3859	16.2080	644.3152	30.0407
791.7657	12.4055	802.9495	18.6512
1068.0566	1.8971	1081.6889	1.9842
1166.5051	3.2166	1152.1859	6.6879
1466.6667	17.7797	1459.5152	39.0757
1638.8687	4.1292	1642.4404	7.6927
1689.6404	4.3910	1686.4404	7.6571
1894.6182	22.5008	1893.4626	33.0378
2000.7434	18.9799	2003.7818	27.4724
2365.0182	21.6032	2367.7010	37.9632
2479.6687	20.9941	2517.3333	40.1630
2715.2727	19.3499	2700.5980	41.2734
2954.4404	11.4821	2937.5919	38.9231
3349.5111	4.7824	3064.6626	27.9120
3443.0788	5.2493	3370.2141	26.3468
3696.7596	15.1767	3457.6242	26.2698
-	-	3540.0727	28.2868
-	-	3697.3818	30.2229
-	-	3802.1172	30.3753

For instance, to improve the performance of the BNS catalyst, additives such as transition metal oxides (e.g., ZnO or TiO_2) can be incorporated, as used by [20]. These additives can introduce new active sites and enhance the catalyst's overall efficiency in biodiesel production. If the BNS catalyst is improved by adding transition metal oxide additives such as ZnO or TiO_2, the FTIR analysis is expected to reveal new peaks corresponding to the functional groups associated with these metal oxides. Typically, these would include metal-oxygen (M-O) stretching vibrations and metal hydroxides (M-OH). Peaks for M-O bonds [21], where M represents Zn, Ti, or other transition metals, are usually observed in the range of 400-700 cm^{-1}, due to the stretching vibrations of the M-O bonds. Likewise, hydroxide groups presence along with the metal oxides [22], leads to the appearance of additional peaks in the range of 3200-3600 cm^{-1}, which are indicative of M-OH stretching vibrations.

3.2 SEM Image

The SEM image of the carbonized Bambara nutshell (BNS) catalyst in Figure 2, which differs from the one realized by [23], reveals essential features that contribute to its catalytic effectiveness for biodiesel production. The surface morphology, as displayed by the SEM, shows a porous structure with high surface area. This porosity is advantageous because it allows for a greater number of active sites to be available for the esterification and transesterification reactions, which are crucial in biodiesel synthesis. The presence of well-distributed pores also enhances the diffusion of reactants, facilitating improved contact between the catalyst and reactant molecules, such as OA and CH_3OH, which ultimately improves reaction efficiency, Together, these morphological characteristics displayed in Figure 3 porosity, high surface area, and rough texture are indicative of an efficient catalyst, capable of achieving optimal conversion rates in FAME production from OA.

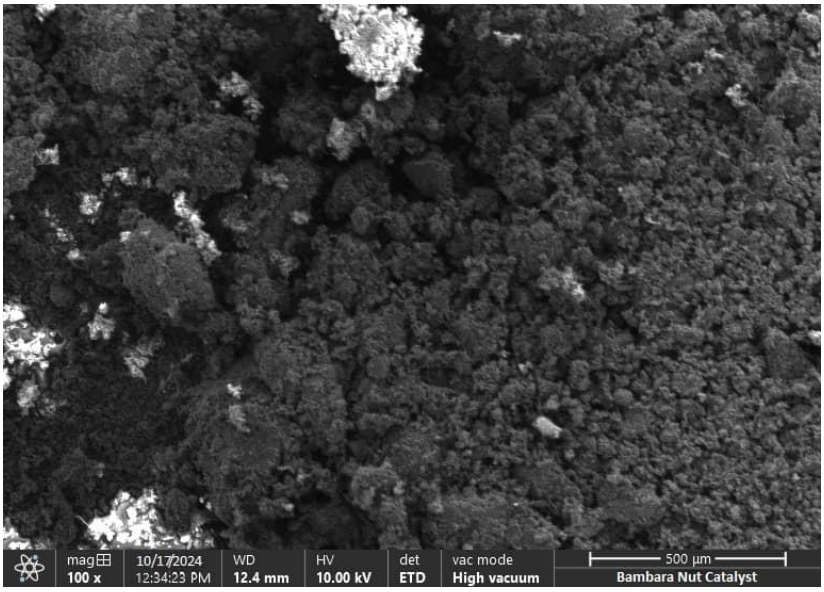

Figure 2. BNC SEM Micrograph

3.3 Regression Model Statistics

In Figure 3, the regression model presents both coded and actual (uncoded) coefficients. Coded coefficients represent the standardized form of the variables according to [24], often normalized to have a mean of zero and a standard deviation of one. This standardization simplifies the interpretation and comparison of coefficients by placing them on a common scale. Uncoded coefficients, on the other hand, reflect the actual units of measurement used in the experiments (e.g., %, min). The differences arise because coded coefficients remove the units (Figure 3a – left), emphasizing relative impacts, while uncoded coefficients retain the units (Figure 3b – left), showing absolute impacts.

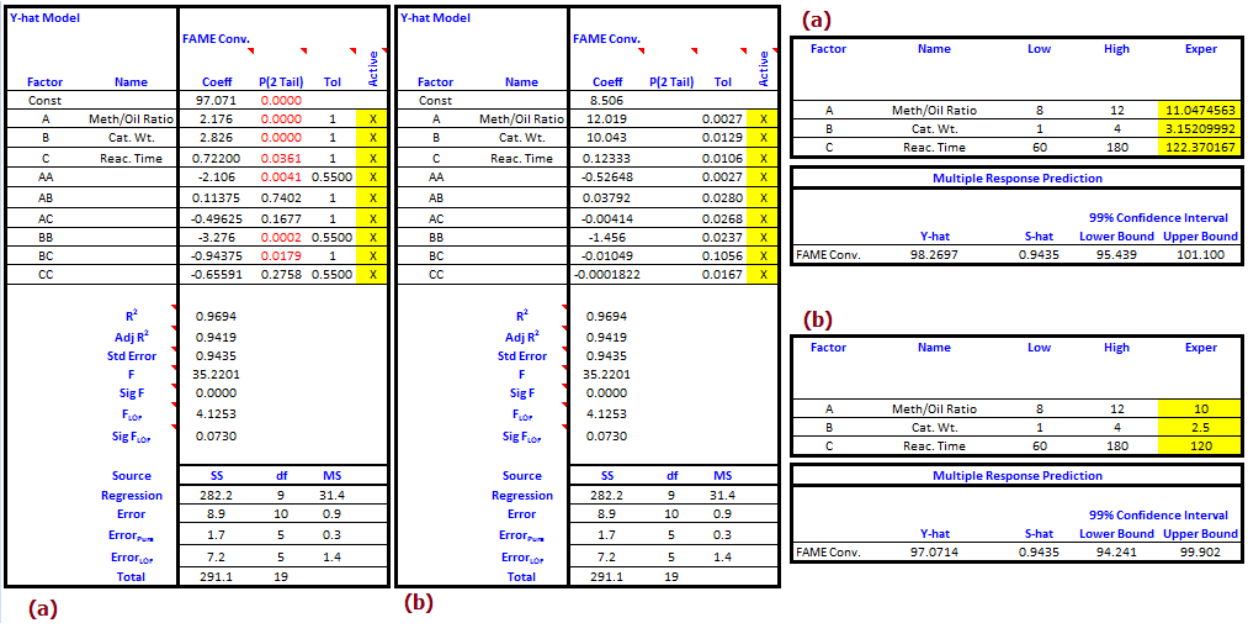

Y-hat Model — FAME Conv.

Factor	Name	Coeff	P(2 Tail)	Tol	Active
Const		97.071	0.0000		
A	Meth/Oil Ratio	2.176	0.0000	1	X
B	Cat. Wt.	2.826	0.0000	1	X
C	Reac. Time	0.72200	0.0361	1	X
AA		-2.106	0.0041	0.5500	X
AB		0.11375	0.7402	1	X
AC		-0.49625	0.1677	1	X
BB		-3.276	0.0002	0.5500	X
BC		-0.94375	0.0179	1	X
CC		-0.65591	0.2758	0.5500	X

R^2	0.9694
Adj R^2	0.9419
Std Error	0.9435
F	35.2201
Sig F	0.0000
F_{LOF}	4.1253
Sig F_{LOF}	0.0730

Source	SS	df	MS
Regression	282.2	9	31.4
Error	8.9	10	0.9
$Error_{Pure}$	1.7	5	0.3
$Error_{LOF}$	7.2	5	1.4
Total	291.1	19	

(a)

Y-hat Model — FAME Conv.

Factor	Name	Coeff	P(2 Tail)	Tol	Active
Const		8.506			
A	Meth/Oil Ratio	12.019	0.0027		X
B	Cat. Wt.	10.043	0.0129		X
C	Reac. Time	0.12333	0.0106		X
AA		-0.52648	0.0027		X
AB		0.03792	0.0280		X
AC		-0.00414	0.0268		X
BB		-1.456	0.0237		X
BC		-0.01049	0.1056		X
CC		-0.0001822	0.0167		X

R^2	0.9694
Adj R^2	0.9419
Std Error	0.9435
F	35.2201
Sig F	0.0000
F_{LOF}	4.1253
Sig F_{LOF}	0.0730

Source	SS	df	MS
Regression	282.2	9	31.4
Error	8.9	10	0.9
$Error_{Pure}$	1.7	5	0.3
$Error_{LOF}$	7.2	5	1.4
Total	291.1	19	

(b)

(a)

Factor	Name	Low	High	Exper
A	Meth/Oil Ratio	8	12	11.0474563
B	Cat. Wt.	1	4	3.15209992
C	Reac. Time	60	180	122.370167

Multiple Response Prediction

	Y-hat	S-hat	99% Confidence Interval Lower Bound	Upper Bound
FAME Conv.	98.2697	0.9435	95.439	101.100

(b)

Factor	Name	Low	High	Exper
A	Meth/Oil Ratio	8	12	10
B	Cat. Wt.	1	4	2.5
C	Reac. Time	60	180	120

Multiple Response Prediction

	Y-hat	S-hat	99% Confidence Interval Lower Bound	Upper Bound
FAME Conv.	97.0714	0.9435	94.241	99.902

Figure 3. Regression Model with (a) Coded and (b) Actual (Uncoded) Coefficients

Significant model parameters and constants are those with p-values <0.05 [25], indicating statistical significance at the 95% confidence level. These coefficients contribute meaningfully to the predictive power of the regression model. Some specific p-values highlighted in red ink (except AB, AC & C^2) indicate

that these values are statistically significant [26] and a visual differentiation helps to quickly identify which coefficients have a significant impact on the model's predictions. Ideally, the model equation used for the fit plot of predicted versus actual response is typically the one with coded coefficients, shown in Figure 4a. Tolerance (Tol) is a measure of multicollinearity in the regression model. It is defined as 1 minus the coefficient of determination value (R^2) when a particular predictor is regressed against all other predictors. Low tolerance values (close to 0, viz., 0.0027-0.028) indicate high multicollinearity, suggesting that the predictor shares a significant amount of variance with other predictors. It can be problematic as it affects the stability and interpretability of the regression coefficients, as displayed on the uncoded data segment of Figure 3b. A high R^2 value (0.9694) indicates a good fit of the model to the data, according to [27]. Adjusted R^2 (0.9419) adjusts the statistic based on the number of predictors in the model, providing a more accurate measure when multiple variables are involved. A standard error (Std Error = 0.9435 or S-hat) indicates the average distance that the observed values fall from the regression line. Lower Std Error value, as in this study, suggests a better fit of the model. It is obviously equal in both coded and uncoded report sheet. High Fisher (F-test) value = 35.2201 indicates that the model is statistically significant as stated in [28], and that the predictors (A, B & C) collectively have a strong relationship with the dependent variable (biodiesel conversion). Sig F p-value (< 0.05) show that the overall model is statistically significant [29, 30]. In other words, there is a very low probability that the observed relationship is due to random chance. The lack of fit F value (F_{LOF}) assesses whether there is significant LOF in the model. A value of 4.1253 is relatively low, suggesting that there may not be significant issues with the model fit. It is also observed that the p-value for Sig F_{LOF} (0.0730) is higher than the conventional alpha level of 0.05. Thus, the LOF is not statistically significant, meaning the model fits the data reasonably well without major deviations. Regression sum of squares (SS) and error SS respectively measures the variation 'explained' and 'not explained' by the model. As evaluated by [31], the mean square (MS) for regression (31.4) reflects the average amount of variability explained by each predictor, whereas the MS for error (0.9) reflects the average variability within the residuals. Pure error ($Error_{Pure}$) SS as reported in [32], represents the pure error without the influence of LOF, where an MS = 0.3 reflects the average variability in such error. $Error_{LOF}$ SS represents the error attributed to LOF, with its MS value of 1.4 reflecting the average variability due to the model's LOF. The predicted FAME conversion (Y-hat) for the coded data is 98.2697% (Figure 3a – right), while for the uncoded data, it is 97.0714% (Figure 3b – right). This indicates that the model's prediction for the FAME conversion is slightly higher when the factors are expressed in coded form. This difference suggests that using coded data may lead to marginally improved predictions, potentially due to the standardization of the factor levels in the coded format. Lastly, for the coded data, the 99% confidence interval (CI) ranges from 95.439 to 101.100, while for the uncoded data, it ranges from 94.241 to 99.902. Such widening and shift in the CI for the coded data may reflect the scaling differences between the coded and uncoded factor levels. Despite these differences, the CIs in both cases are reasonably tight, indicating a high degree of confidence in the accuracy of the predictions. Figure 4 presents the marginal means plot for the FAME conversion under varying conditions of CH_3OH/oil ratio, catalyst weight, and reaction time. Each subplot shows the interaction effects and the marginal means of these variables. The top-left plot shows the marginal means of FAME conversion against the CH_3OH/oil ratio. The conversion increases from 92% at a ratio of 8:1 to about 98.27% at a ratio of 10:1, then slightly declines at a ratio of 12:1. Top-center plot depicts the interaction between CH_3OH/oil ratio and catalyst weight, indicating the highest FAME conversion at a CH_3OH/oil ratio of 10:1 across all catalyst weights. Specifically, a catalyst weight of 2.5 wt.% yields the highest conversion. While the top-right plot illustrates that FAME conversion increases with reaction time, peaking at 120 min and then slightly dropping at 180 min for all CH_3OH/oil ratios.

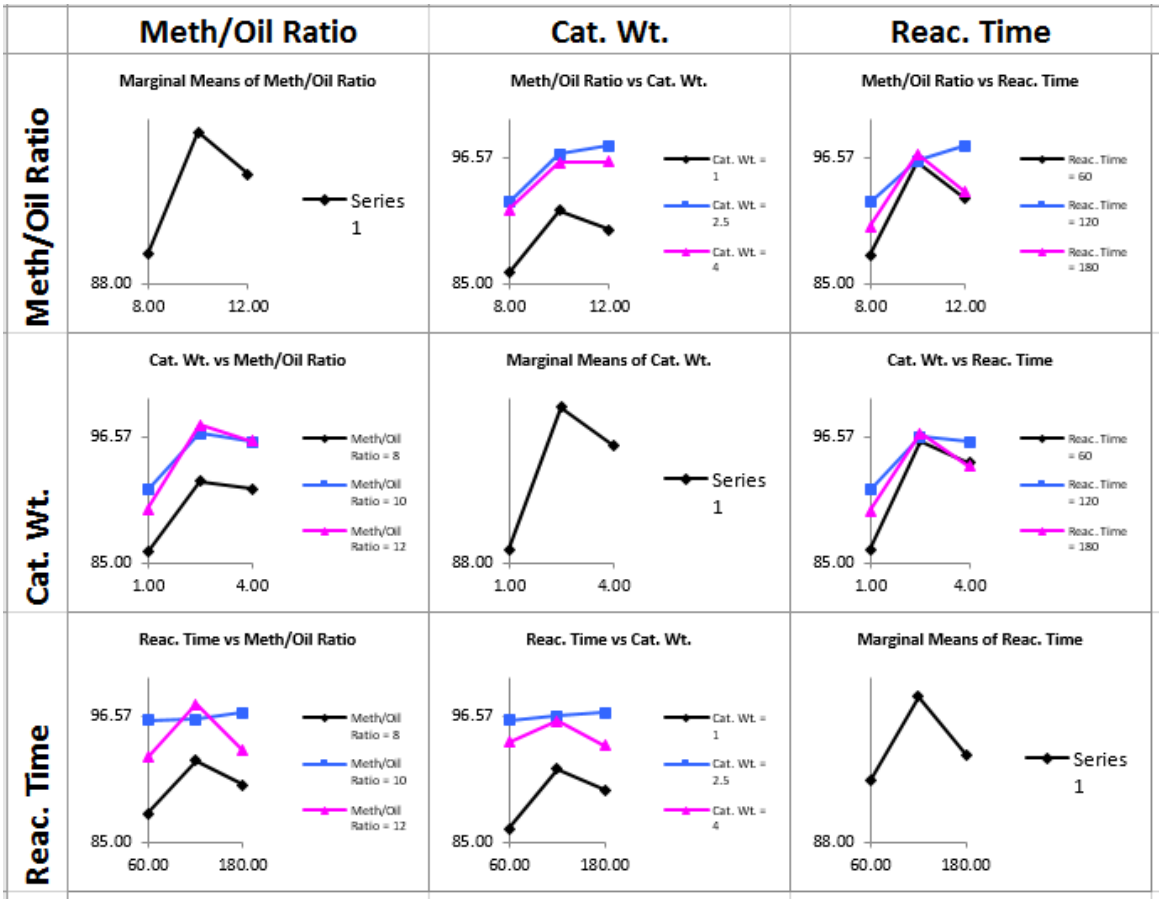

Figure 4. Marginal Means Plot for the FAME Conversion

Middle-left plot of Figure 4 displays the interaction between catalyst weight and CH_3OH/oil ratio. It shows that the FAME conversion is maximized at a catalyst weight of 2.5 wt.% and a CH_3OH/oil ratio of 10:1. The middle-center plot shows the marginal means of FAME conversion against catalyst weight. The conversion increases from 90% at 1% catalyst weight to around 98.27% at 2.5 wt.% catalyst weight, then drops slightly at 4%. Lastly, the middle-right plot reveals that the FAME conversion peaks at a catalyst weight of 2.5 wt.% for reaction times of 60 and 120 min, with a slight decline at 180 min. On the other hand, the bottom-left plot shows the interaction between reaction time and CH_3OH/oil ratio. Highest FAME conversion occurs at 120 min for all CH_3OH/oil ratios, with the CH_3OH/oil ratio of 10:1 consistently yielding the highest conversion. In the bottom-center plot, the interaction between reaction time and catalyst weight was displayed. Similar to the previous observations, the highest conversion occurs at 120 min across all catalyst weights, with a catalyst weight of 2.5 wt.% giving the highest conversion. The bottom-right plot shows the marginal means of FAME conversion against reaction time. The conversion increases from 94% at 60 min to around 98.27% at 120 min, then decreases slightly at 180 min. Generally, the marginal means plot indicates that the optimal conditions for FAME conversion are a CH_3OH/oil ratio of 10:1, a catalyst weight of 2.5 wt.%, and a reaction time of 120 min. These conditions consistently yield the highest conversion rates across the various interactions depicted in the plots. [33] also reported a single-parameter interaction in his study.

3.4 3D Surface, Interaction and Contour Plots Analysis

Plots in Figures 5 (specifically, a & d) shows a curved surface indicating a nonlinear relationship between the CH_3OH/oil ratio and catalyst weight concerning FAME conversion (termed response value). They both reveal that the conversion rate increases with the CH_3OH/oil ratio up to a certain point, after which it stabilizes or decreases slightly. Similarly, an increase in catalyst weight also boosts conversion

rates until an optimal point is reached (2.5 wt.%), beyond which the conversion may not significantly improve or might even decline slightly. Figure 5 shows the Response Surface Curve and Plots for A-B Combined Effect.

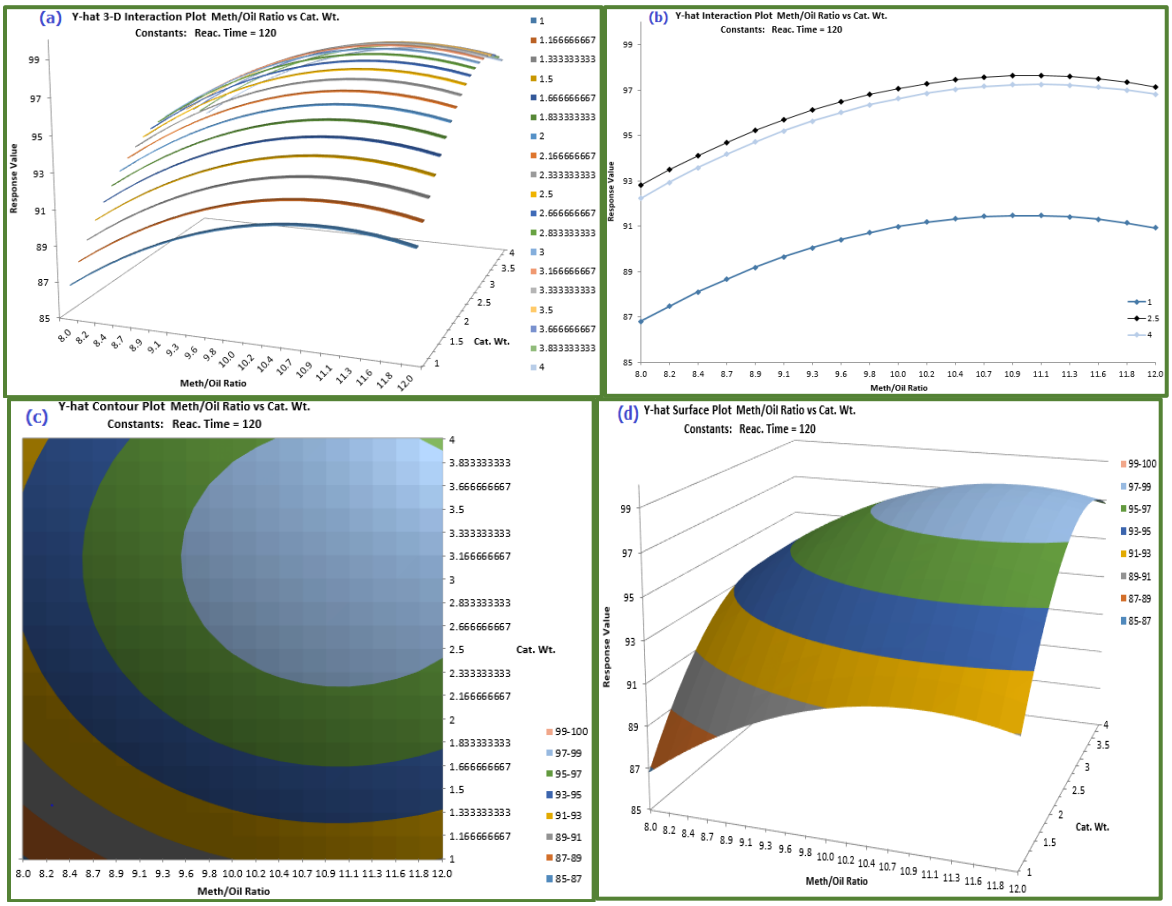

Figure 5. Response Surface Curve and Plots for A-B Combined Effect

Obviously, as the CH_3OH/oil ratio increases from 8:1 to 11:1, the FAME conversion percentage also increases. Beyond 11:1, the conversion rate starts to plateau or slightly decrease, indicating that a CH_3OH/oil ratio higher than 11:1 does not significantly enhance the conversion. Increasing the catalyst weight from 1 to around 2.5 wt.% results in higher FAME conversion (attaining between 97-99%), showcased by the sky-blue region in Figure 5d. However, beyond 2.5 wt.%, further increase in catalyst weight do not significantly improve the conversion rate and may even cause a slight decline, as mentioned in the foregone, as well as in [34]. Beyond the optimal points, there are diminishing returns on FAME conversion, indicating the importance of optimizing these parameters rather than simply increasing them. [20] obtained a FAME conversion of 80% for A-B interaction. Interactive plot in Figure 5b shows how varying the CH_3OH/oil ratio and catalyst weight simultaneously affects the FAME conversion, especially the black trending line standing taller than the light and dark blue lines. The density of the colored contour lines indicates regions of rapid change in FAME conversion [31]. Tightly packed lines suggest steep changes, while widely spaced lines indicate more gradual changes. Area with the most closely packed contour lines at the highest Z-values is where the highest FAME conversion is achieved is located. It is almost a circular sky-blue region in Figure 6c. Densely concentrated regions in the 3D-interaction, contour and 3D surface plots, are also shown in Figures 6 and 7 (a, c & d), by specific colors.

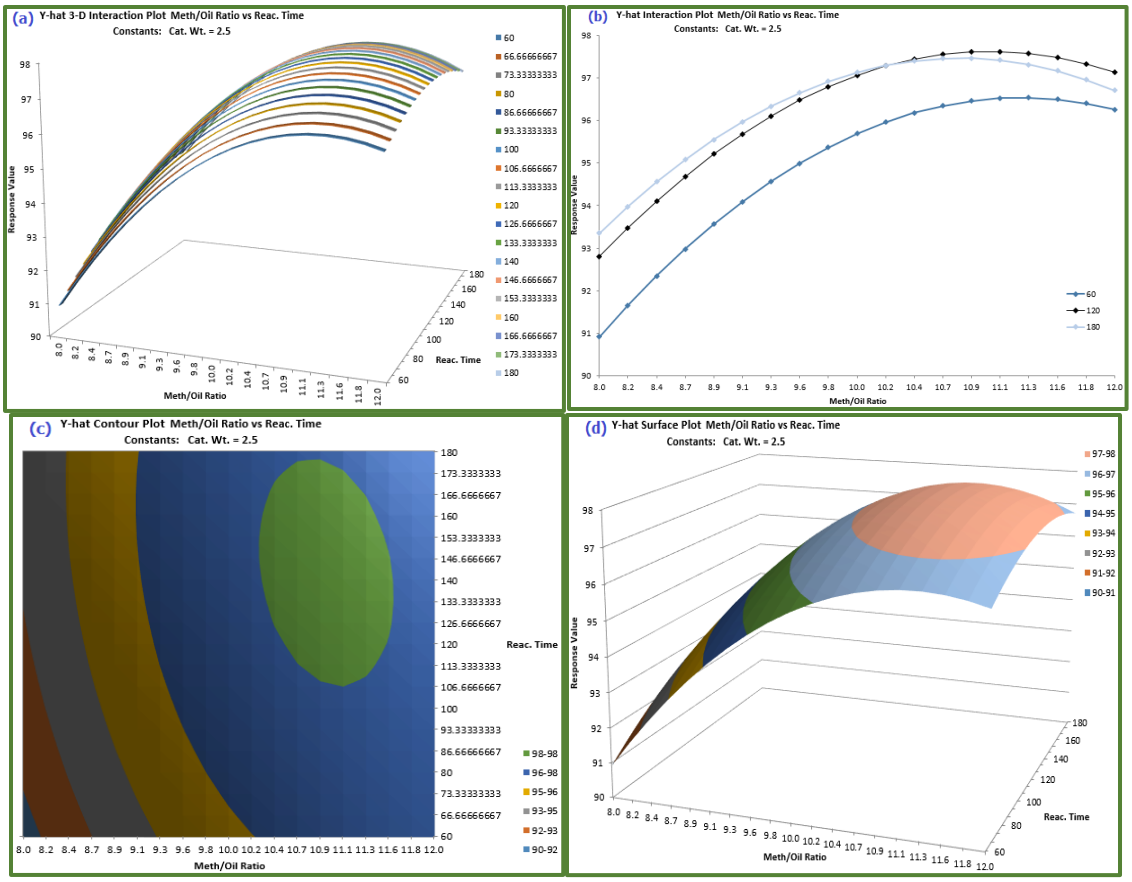

Figure 6. Response Surface Curve and Plots for A-C Combined Effect

Using the same idea, the optimal combinations derived from Figure 6 are 120 min reaction time (Figure 6b), 11.05:1 CH_3OH/oil ratio and 97.98% FAME conversion. The surface plot (Figure 7a & 7d) shows that as the CH_3OH/oil ratio increases, the FAME conversion rate increases up to a certain point, as observed in [33] and 30]. Similarly, increasing the reaction time also enhances the conversion rate to an optimal point, beyond which the benefits taper off [28]. In Figure 6c, a 2D view with lines/shades of constant response (FAME conversion) drawn on the graph, is shown. Lines closer together indicate steep changes in conversion rates, while lines farther apart suggest more gradual changes (Figure 7a). B-C combined effect on biodiesel conversion is showcased by Figure 7. Curved surface of Figure 7 (a & d) is an indication of a nonlinear relationship between catalyst weight, reaction time, and FAME conversion. A 2D representation of the contour line in Figure 7c, shows lines of constant biodiesel conversion, demonstrated by varying color patterns. Tighter blue contour region is the point where there are steep changes in FAME efficiency. It is observed that the optimal catalysts weight and reaction time are respectively, 2.5 wt.% and 120 min (Figure 7b), corresponding to a conversion of 97.50%. Figures 7d & 7d 3D surface plots are almost identical compared to Figure 6d, were there is spread in the area covered by the 3D curved region. In consonance with what was obtained by [35], FAME conversion increased when the reaction time and catalyst loading increased and decreased slightly after the optimum value is achieved. Obviously, Figures 5 and 7 are alternative confirmations to individual relationships explained in Figure 5. Ultimately, the 3 process variables are highly sensitive to biodiesel generation.

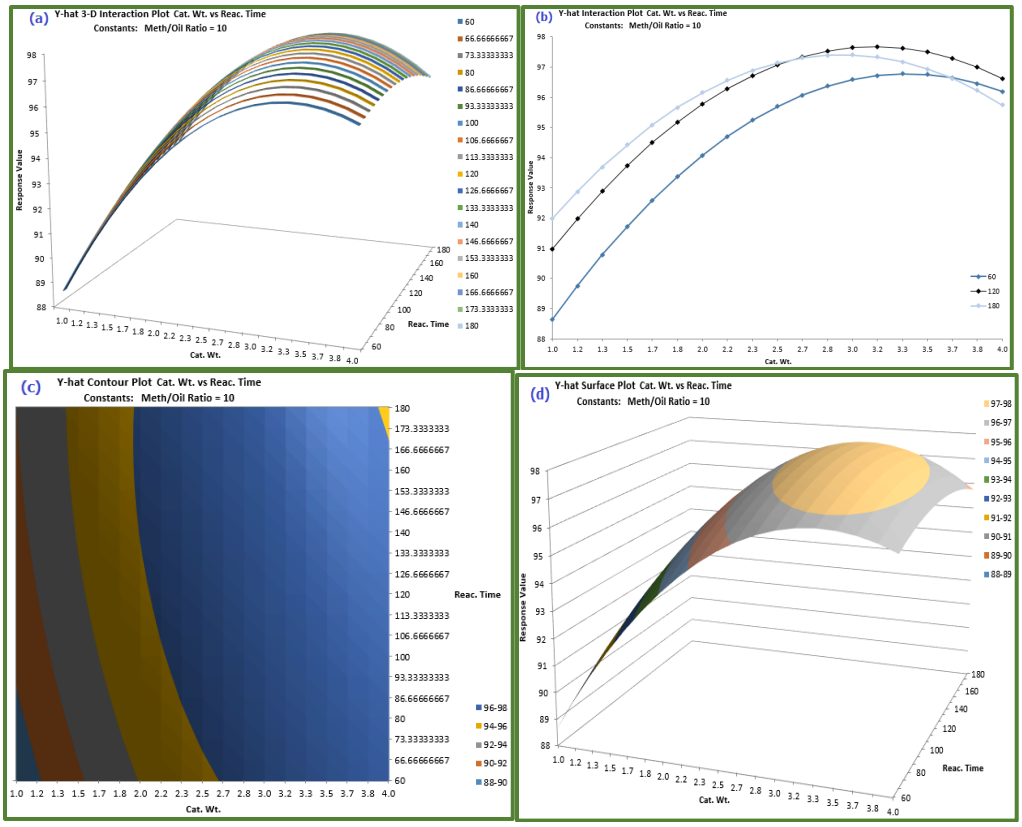

Figure 7. Response Surface Curve and Plots for B-C Combined Effect

3.5 Pareto Chart and Optimal Combinations

Y-hat Pareto chart in Figure 8 is a graphical representation of the effects of various factors on FAME conversion. Each bar in the Pareto chart represents a coefficient associated with a particular factor or interaction of factors in the regression model. The length of each bar indicates the magnitude of the effect of that factor on FAME conversion.

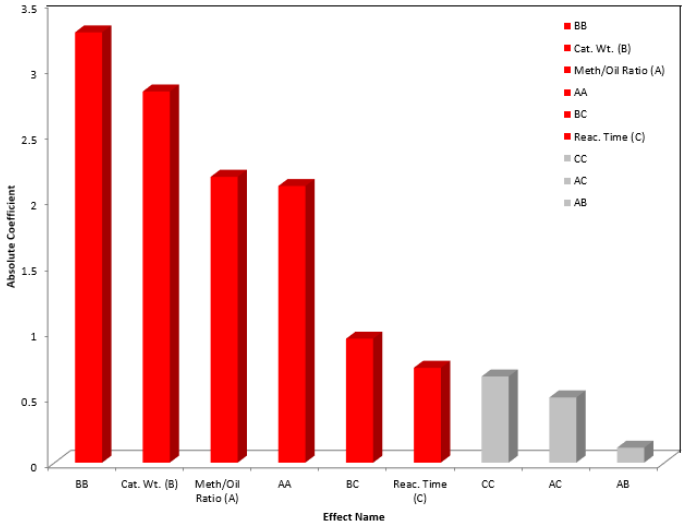

Figure 8. Y-hat Pareto of Coefficients-FAME Conversion

A, B, A^2 and B^2 are tall bars, pointing to significant factors. Essentially, these factors have the tallest bars, indicating they have the most substantial impact on FAME conversion. Changes in these factors lead to significant changes in the conversion rate. While still impactful, short bars of AB, AC, C^2, C and

BC, indicates that changes in these parameters have a less pronounced effect on FAME conversion. Combined effect of two factors for tall and short bars (significant and non-significant), highlights the importance of optimizing both factors together rather than in isolation. Factors with p-values <0.05 are considered statistically significant at the 95% CI. These are usually highlighted in red ink, and cut-across the two categories of significance. In Figure 9, A and B should be prioritized during the optimization process due to their significant impact on FAME conversion [36]. Even though C is also important, it should be optimized after the primary factors. Earlier, the optimal combinations provided by Figures 4 to 7 are based on two process condition interaction with the biodiesel conversion. DOE Pro XL gives the 3-parameter optimal combination. For maximum biodiesel conversion of up to 98.27%, the catalyst load, CH_3OH/oil ratio and reaction time of 3.15 wt.%, 11.05:1 and 122.37 min, respectively, should be employed. Practical examination gives a conversion of 96.06%, closer to the software value.

3.6 Residual Analysis

Among the 20-run DOE given by the factorial design described in [24], a response value of 97.63% actual (or 97.14% predicted) at 2.5 wt.%, 120 min, 12:1 ratio and 65℃ temperature was realized. An indication that the quadratic coefficient/model in Figure 4 satisfy the empirical values, are the closer estimate of the predicted biodiesel conversion compared to the actual ones (Table 2). Leverage measures the influence of each data point on the fitted values of the regression model. In Table 2, the leverage values vary between 0.118 and 0.793, where higher leverage values (around 0.793) suggest points having more influence on the regression model compared to those with lower leverage. Studentized residual (SR) is the residual divided by an estimate of its standard deviation. Negative values indicate that the observed values are below the predicted values, and positive values indicate they are above. The range of these values is from -1.881 to 2.669, which suggests that some points have substantial deviations from the fitted line, especially those with higher absolute values.

Table 2. Residual Data and Predicted Response Values

Y-hat Residuals				FAME Conv.						
	Design Values							Studentized	R-Studentized	
Run #	Meth/Oil Ratio	Cat. Wt.	Reac. Time	Actual Y	Predicted Y	Leverage	Residual	Residual	Residual	Cook's D
1	8	1	180	87.5	88.3073864	0.793182	-0.80739	-1.88165588	-2.221090926	1.35789
2	8	4	60	90.63	91.2953864	0.793182	-0.66539	-1.5507175	-1.68803787	0.92225
3	10	2.5	120	96.98	97.0713636	0.118182	-0.09136	-0.1031186	-0.097878946	0.00014
4	10	2.5	120	96.02	97.0713636	0.118182	-1.05136	-1.18663343	-1.214487915	0.01887
5	12	4	180	94.75	95.4313864	0.793182	-0.68139	-1.58800633	-1.742103307	0.96714
6	8	4	180	92.99	91.8443864	0.793182	1.14561	2.66991212	4.726705815	2.73387
7	8	2.5	120	92.48	92.7894545	0.490909	-0.30945	-0.45967655	-0.440769106	0.02038
8	10	4	120	96.06	96.6214545	0.490909	-0.56145	-0.83400774	-0.82025035	0.06707
9	8	1	60	84.62	83.9833864	0.793182	0.63661	1.483661166	1.593835507	0.84422
10	10	2.5	120	96.8	97.0713636	0.118182	-0.27136	-0.30627763	-0.29193295	0.00126
11	10	2.5	180	96.86	97.1374545	0.490909	-0.27745	-0.41214243	-0.394356276	0.01638
12	10	2.5	120	97.63	97.0713636	0.118182	0.55864	0.630511232	0.610411812	0.00533
13	10	2.5	120	97.06	97.0713636	0.118182	-0.01136	-0.0128257	-0.012167624	2.2E-06
14	10	2.5	60	96.15	95.6934545	0.490909	0.45655	0.67817145	0.65869546	0.04435
15	12	1	60	87.91	89.1003864	0.793182	-1.19039	-2.77425729	-5.483706625	2.95174
16	12	4	60	97.63	96.8673864	0.793182	0.76261	1.777310715	2.038541372	1.21146
17	10	2.5	120	97.58	97.0713636	0.118182	0.50864	0.574078169	0.553820845	0.00442
18	10	1	120	91.71	90.9694545	0.490909	0.74055	1.100036765	1.113104697	0.11669
19	12	1	180	92.06	91.4393864	0.793182	0.62061	1.446372335	1.543006788	0.80231
20	12	2.5	120	97.63	97.1414545	0.490909	0.48855	0.72570557	0.707342718	0.05078

R-Studentized Residual (RSR) is similar to the SR but is adjusted for the leverage of each point. It ranged from -5.484 to 4.727, showing significant deviations from the regression model, particularly in cases with high leverage. Cook's D measures the influence of each data point on the fitted values of the regression model. A higher Cook's D value indicates a more influential data point and the reported values ranged from 0.00014-2.952. High Cook's D values (e.g., 2.952) suggest that these points have a substantial impact on

the regression results, indicating potential outliers or influential points that might need further investigation. Data points with high leverage values (close to 0.793) often correspond with larger RSR and higher Cook's D values. This indicates that points with high leverage can have large residuals and a significant impact on the model [37]. For instance, a point with leverage of 0.793, an RSR of -5.484, and a Cook's D value of 2.952 shows a strong influence on the model. Points with extreme residuals (both positive and negative) tend to have higher Cook's D values. Correlation of such, suggests that outliers with large deviations from the fitted line often have more influence on the regression results. Lastly (Table 2), points with high leverage tend to have higher Cook's D values. High leverage points are more likely to influence the model, which aligns with having higher Cook's D values. For example, high leverage points often have significant Cook's D values, indicating their potential impact on the regression analysis [37].

3.7 Biodiesel Conversion Model and Fit

Sufficient experimental and analytical data resulted in an R^2 value of 0.9694, a good predicted response (Figure 9), significant impacts, statistical performance and correct optimal combinations. It resulted in the predicted biodiesel model in terms of coded (Equation 3) and actual factors (Equation 4).

$$\text{FAME Conv. (\%)}_{\text{Coded}} = \begin{Bmatrix} 97.071 + 2.176A + 2.826B + 0.722C - 2.106A^2 + \\ 0.11375AB - 0.49625AC - 3.276B^2 - 0.94375BC \\ -0.65591C^2 \end{Bmatrix} \quad (3)$$

$$\text{FAME Conv. (\%)}_{\text{Actual}} = \begin{Bmatrix} 8.506 + 12.019A + 10.043B + 0.12333C - 0.52648A^2 \\ +0.03792AB - 0.00414AC - 1.456B^2 - 0.01049BC \\ -0.0001822C^2 \end{Bmatrix} \quad (4)$$

Equations 3 and 4 are quadratic model equation in terms of A, B and C factors, which can be used to predict the conversion of biodiesel within the ranges specified in the study. Similar parameter combination has been rarely reported in previous studies. Evidently, upon fitting the experimental versus correlated biodiesel efficiency, there was only 3.06% non-fitted points, as shown in Figure 9. Based on that, the BNS catalyst performance in converting the oleic fatty acid to biodiesel is satisfactory.

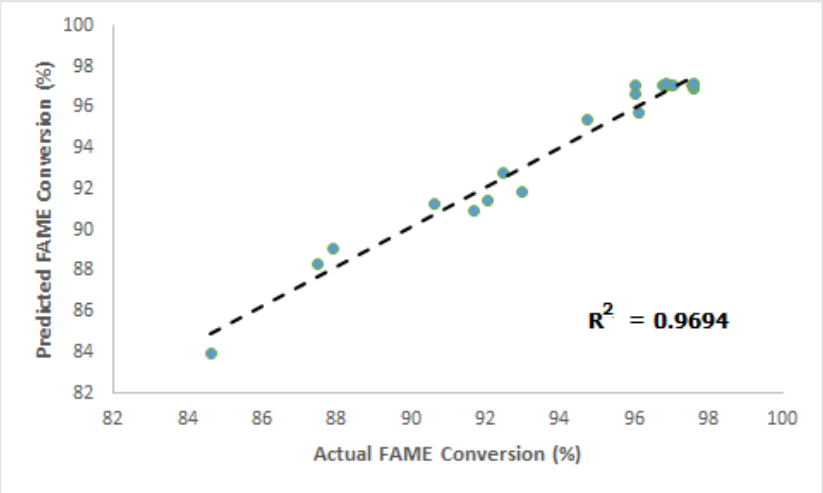

Figure 9. Predicted Versus Actual Response Fit

4 CONCLUSIONS

Seemingly, all the parameters varied, i.e., A (methanol/oil ratio): 8-12:1, B (catalyst loading): 1-4 wt.% and C (reaction time): 60-180 min at 65℃, significantly affect the response variable (biodiesel conversion), as illustrated by the 3D surface, 2D interaction and contour plots. The Y-hat Pareto chart effectively highlights the most influential factors in the biodiesel production process. Methanol/oil ratio and catalyst weight are the key drivers of FAME conversion using BNS as catalyst, and their optimization

is crucial for maximizing the conversion. Though, the optimum factors are 3.15 wt.% catalyst weight, 11.05:1 CH_3OH/oil ratio and 122.37 min esterification reaction period at 98.27%, which is almost in line with the empirical test-run value of 96.06%. Clearly, the quadratic model describing the process proved that BNS heterogenous catalyst was an effective catalyst for the continuous esterification with CH_3OH and OA. Residual analysis from the DOE Pro XL v.21 (Serial Number: DP-6960-690111) shows that points with lower leverage and Cook's D values typically have less impact on the model and exhibit smaller residuals. While FTIR analysis provides crucial information about the functional groups present and SEM, the surface morphology, additional characterization techniques like X-ray diffraction (XRD) for crystallinity and Brunauer-Emmett-Teller (BET) analysis for surface area is recommended to fully understand the catalyst's properties.

REFERENCES

1. Ben-Iwo, J., Manovic, V. and Longhurst, P. (2016). Biomass resources and biofuels potential for the production of transportation fuels in Nigeria. *Renew. Sustain. Energy Rev*., vol. 63, pp. 172-192.
2. He, B.B., Thompson, J.C., Routt, D.W. and Van Gerpen, J.H. (2006). Moisture distribution in biodiesel and its fossil diesel blend. *In Paper number 066141, 2006 ASAE Annual Meeting*.
3. He, B.B., Singh, A.P. and Thompson, J.C. (2005). Experimental optimization of a continuous-flow reactive distillation reactor for biodiesel production. *Trans. ASAE*, vol. 48, no. 6, pp. 2237-2243.
4. He, B.B., Singh, A.P. and Thompson, J.C. (2007). Function and performance of a pre-reactor to a reactive distillation column for biodiesel production. *Trans. ASABE*, vol. 50, no. 1, pp. 123-128.
5. He, B.B., Thompson, J.C., Routt, D.W. and Van Gerpen, J.H. (2007). Moisture absorption in biodiesel and its petro-diesel blends. *Appl. Eng. Agric*., vol. 23, no. 1, pp. 71-76.
6. Singh, A.P., He, B.B., Thompson, J.C. and Van Gerpen, J.H. (2006). Process optimization of biodiesel production using alkaline catalysts. *Appl. Eng. Agric*., vol. 22, no. 4, pp. 597-600.
7 Thompson, J.C. and He, B.B. (2007). Biodiesel production using static mixers. *Trans. ASABE*, vol. 50, no. 1, pp. 161-165.
8. Abubakar, A.M., Kefas, H.M., Luka, Y. and Kawuwa, J.J. (2024). Revolutionalizing biodiesel synthesis: Kinetic and thermodynamic insights with carbonized doum-shell catalyst. *Trends Ecol. Indoor Environ. Eng.*, vol. 2, no. 2, pp. 11-23.
9. Kefas, H.M., Kovo, A.S., Odo, G. and Abdulkareem, A.S. (2022). Synthesis of hierarchical zeolite Y catalyst for the production of biodiesel from waste vegetable oil. *Niger. J. Eng. Sci. Technol. Res*., vol. 8, no. 1, pp. 57-65.
10. Tat, M.E., Wang, P.S., Van Gerpen, J.H. and Clemente, T.E. (2007). Exhaust emissions from an engine fueled with biodiesel from high-oleic soybeans. *J. Am. Oil Chem. Soc*., vol. 84, pp. 865-869.
11. Sattari, S., Vahabzadeh, F. and Aghtaei, H.K. (2015). Performance of loofa-immobilized Rhizopus oryzae in the enzymatic production of biodiesel with use of oleaic acid in n-hexane medium. *Brazilian J. Chem. Eng.*, vol. 32, no. 2, pp. 367-376.
12. Wang, Y., Wang, D., Tan, M., Jiang, B., Zheng, J., Tsubaki, N. and Wu, M. (2015). Monodispersed hollow SO3H-functionalized carbon/silica as efficient solid acid catalyst for esterification of oleic acid. *Appl. Mater. Interfaces*, pp. 1-20.
13. Kumawat, M.K. and Rokhum, S.L. (2022). Biodiesel production from oleic acid using biomass-derived sulfonated orange peel catalyst. *Front. Catal*., vol. 2, no. 914670, pp. 1-12.

14. Yusuff, A.S., Thompson-Yusuf, K.A. and Porwal, J. (2022). Sulfonated biochar catalyst derived from eucalyptus tree shed bark: Synthesis, characterization and its evaluation in oleic acid esterification. *RSC Adv*., vol. 12, pp. 10237-10248.

15. Shu, Q., Tang, G., Liu, F., Zou, W., He, J., Zhang, C. and Zou, L. (2017). Study on the preparation, characterization of a novel solid Lewis acid Al3+-SO42−/ MWCNTs catalyst and its catalytic performance for the synthesis of biodiesel via esteri fi cation reaction of oleic acid and methanol. *Fuel*, vol. 209, pp. 290-298.

16. Rafiee, E. and Mirnezami, F. (2016). Temperature regulated Brønsted acidic ionic liquid-catalyze esterification of oleic acid for biodiesel application. *J. Mol. Struct*., pp. 1-27.

17. Mahmoud, H.R. (2019). Bismuth silicate (Bi4Si3O12 and Bi2SiO5) prepared by ultrasonic-assisted hydrothermal method as novel catalysts for biodiesel production via oleic acid esterification with methanol. *Fuel*, vol. 256, no. 115979, pp. 1-10.

18. Ghorbani-Choghamarani, A., Taherinia, Z. and Tyula, Y.A. (2022) Efficient biodiesel production from oleic and palmitic acid using a novel molybdenum metal–organic framework as efficient and reusable catalyst. *Sci. Rep.*, vol. 12, no. 10338, pp. 1-12.

19. Zhou, K. and Chaemchuen, S. (2017). Metal-organic framework as catalyst in esterification of oleic acid for biodiesel production. *Int. J. Environ. Sci. Dev*., vol. 8, no. 4, pp. 5-8.

20. Sabzevar, A.M., Ghahramaninezhad, M. and Shahrak, M.N. (2020). Enhanced biodiesel production from oleic acid using TiO2-decorated magnetic ZIF-8 nanocomposite catalyst and its utilization for used frying oil conversion to valuable product. *Fuel*, pp. 1-15.

21. Junior, J.L.S., Nobre, F.X., De Freitas, F.A., De Carvalho, T.A.F., De Barros, S.S., Nascimento, M.C., Manzato, L., Matos, J.M.E., Brito, W.R., Leyet, Y. and Couceiro, P.R.C. (2021). Copper molybdate synthesized by sonochemistry route at room temperature as an efficient solid catalyst for esterification of oleic acid. *Ultrason. Sonochem*., vol. 73, no. 105541, pp. 1-11.

22. Yin, P., Chen, W., Liu, W., Chen, H., Qu, R., Liu, X., Tang, Q. and Xu, Q. (2013). Efficient bifunctional catalyst lipase/organophosphonic acid-functionalized silica for biodiesel synthesis by esterification of oleic acid with ethanol. *Bioresour. Technol*., vol. 140, pp. 146-151.

23. Odeniyi, M.A., Omoteso, O.A. and Adebisi, A.O. (2017). Solid state characterization and rheological properties of native and modified Bambara groundnut (Vigna subterranean) starches. *J. Excipients Food Chem.*, vol. 8, no. 3, pp. 42–51.

24. Bradley, N. (2007). The Response Surface Methodology. *Degree of Masters of Science in Applied Mathematics and Computer Science, Department of Mathematical Sciences, Indiana University of South Bend*, 2007. [Online]. Available: https://clas.iusb.edu/math-compsci/_prior-thesis/NBradley_thesis.pdf.

25. Saengprachum, N., Cai, D., Li, M., Li, L., Lin, X. and Qiu, T. (2019). Acidic chitosan membrane as an efficient catalyst for biodiesel production from oleic acid. *Renew. Energy*, vol. 143, pp. 1488-1499.

26. Roman, F.F., Ribeiro, A.E., Queiroz, A., Lenzi, G.G., Chaves, E.S. and Brito, P. (2019). Optimization and kinetic study of biodiesel production through esterification of oleic acid applying ionic liquids as catalysts. *Fuel*, vol. 239, pp. 1231-1239.

27. Nguyen, H.C., Huong, D.T.M., Juan, H.Y., Su, C.H. and Chien, C.C. (2018). Liquid lipase-catalyzed esterification of oleic acid with methanol for biodiesel production in the presence of superabsorbent polymer: Optimization by Using Response Surface Methodology. *Energies*, vol. 11, no. 1085, pp. 1-12.

28. Fauzi, A.H.M. and Saidina Amin, N.A. (2013). Optimization of oleic acid esterification catalyzed by ionic liquid for green biodiesel synthesis. *Energy Convers. Manag*., vol. 76, pp. 818-827.

29. Yin, P., Chen, L., Wang, Z., Qu, R., Liu, X., Xu, Q. and Ren, S. (2012). Biodiesel production from esterification of oleic acid over aminophosphonic acid resin D418. *Fuel*, vol. 102, pp. 499-505.

30. Marzouk, N.M., El Naga, A.O.A., Younis, S.A., Shaban, S.A., El Torgoman, A.M. and El Kady, F.Y. (2021). Process optimization of biodiesel production via esterification of oleic acid using sulfonated hierarchical mesoporous ZSM-5 as an efficient heterogeneous catalyst. *J. Environ. Chem. Eng*., vol. 9, no. 105035, pp. 1-16.

31. Yin, P., Chen, L., Wang, Z., Qu, R., Liu, X. and Ren, S. (2012). Production of biodiesel by esterification of oleic acid with ethanol over organophosphonic acid-functionalized silica. *Bioresour. Technol*., vol. 110, pp. 258-263.

32. Ren, H., Li, Y., Du, W. and Liu, D. (2013). Free lipase-catalyzed esterification of oleic acid for fatty acid ethyl ester preparation with Response Surface Optimization. *J. Am. Chem. Soc*., vol. 90, pp. 73-79.

33. Han, B., Yin, F., Liu, S., Zhao, X., Liu, J., Wang, C., Yang, H. and Zhang, W. (2019). Optimization of oleic acid esterification for biodiesel production using Brønsted acidic ionic liquid as a catalyst. *Chiang Mai J. Sci*., vol. 46, no. 4, pp. 714-726.

34. Liu, W., Yin, P., Liu, X. and Qu, R. (2014). Design of an effective bifunctional catalyst organotriphosphonic acid-functionalized ferric alginate (ATMP-FA) and optimization by Box–Behnken model for biodiesel esterification synthesis of oleic acid over ATMP-FA. *Bioresour. Technol*., vol. 173, pp. 266-271.

35. Siti eda eliana Misi, W., Wan Omar, N.N. and Amin, N.A.S. (2010). Heterogeneous esterification of free fatty acid to biodiesel. *Journal-The Inst. Eng. Malaysia*, vol. 71, no. 3, pp. 35-45.

36. Nurhayati, N., Anita, S., Amri, T.A. and Muhdarina, M. (2018). The effects of catalyst weight and mole ratio of oil-methanol on crude palm oil (CPO) esterification using H2SO4 (3M)/clay catalyst. *J. Phys. Conf. Ser*., vol. 1093, no. 012006.

37. McDonald, B. (2002). A teaching note on Cook's Distance - A guideline. *Res. Lett. Inf. Math. Sci*., vol. 3, pp. 127-128.